A new approach to treat tissue destruction in periodontitis with chemically modified dextran polymers

Q. ESCARTIN,*,† C. LALLAM-LAROYE,* B. BAROUKH,* F. O. MORVAN,*,† J. P. CARUELLE,† G. GODEAU,* D. BARRITAULT,† AND J. L. SAFFAR*,[1]

*Laboratoire de Biologie et Physio*P*athologie Crânio-Faciales, Faculté de Chirurgie Dentaire, Université René Descartes (Paris-5), 92120 Montrouge, France; and †Laboratoire CRRET, CNRS FRE 2412, Faculté des Sciences, Université Paris-XII Val de Marne, 94010 Créteil, France

ABSTRACT **Periodontitis are diseases of the supportive tissues of the teeth provoked by bacteria and characterized by gingival inflammation and bone destruction. We have developed a new strategy to repair tissues by administrating agents (RGTA) that mimic heparan sulfates by protecting selectively some of the growth factors naturally present within the injured tissue and interfering with inflammation. After periodontitis induction in hamsters, the animals were left untreated or received weekly i.m. injections of RGTA1507 at a dose of 100 μg/kg, 400 μg/kg, 1.5 mg/kg, or 15 mg/kg for 4 wk. RGTA treatment significantly reduced gingival tissue inflammation, thickened the pocket epithelium by increasing cell proliferation, and enhanced collagen accumulation in the gingiva. A marked reduction in bone loss was observed, resulting from depression of osteoclasia and robust stimulation of bone formation at the dose of 1.5 mg/kg. RGTA treatment for 8 wk at this dose reversed macroscopic bone loss, sharply contrasting with the extensive bone destruction in the untreated animals. RGTA treatment decreased gelatinase A (MMP-2) and B (MMP-9) proforms in gingival tissues. Our data indicate that a 4 wk treatment dose-dependently attenuated gingival and bone manifestations of the disease, whereas a longer treatment restored alveolar bone close to controls. By modulating and coordinating host responses, RGTA has unique therapeutic properties and is a promising candidate for the treatment of human periodontitis.—Escartin, Q., Lallam-Laroye, C., Baroukh, B., Morvan, F. O., Caruelle, J. P., Godeau, G., Barritault, D., Saffar, J. L. A new approach to treat tissue destruction in periodontitis with chemically modified dextran polymers. *FASEB J.* 17, 644–651 (2003)**

Key Words: RGTA · periodontal destruction · gingival inflammation · bone loss · tissue restructuring · osteoprogenitor cells · osteoclasts

PERIODONTITIS AFFECTS the supportive tissues of the teeth (gingiva, cementum, periodontal ligament, and alveolar bone). It affects ~85% of the population to various degrees (1) and can have severe systemic complications (2). Periodontitis can be considered to result from an imbalance between destruction and repair of periodontal tissues, triggered by bacteria present in periodontal pockets and possibly aggravated by systemic disorders. In fact, the bulk of tissue destruction is caused by host responses to oral bacteria (3, 4): host cells (both resident and recruited from blood) release enzymes and cytokines in response to bacterial products.

For decades the treatment of periodontitis has been mainly surgical, but better knowledge of the biological mechanisms responsible for periodontium destruction is leading to an increasing number of medical approaches. Agents potentially active on the inflammatory components of the disease have been assessed in various animal models and in the clinical setting. Anti-inflammatory drugs are particularly effective in controlling tissue destruction (5–7). Cyclines, both with and without antibacterial properties, have been successfully tested for their anti-metalloproteinase actions (8, 9). However, these agents do not reverse bone destruction.

In previous work, we found that a family of compounds designed as mimetics of heparan sulfates toward heparin binding growth factors (HBGF) in vitro could stimulate tissue repair in vivo. These compounds were designated RGTA, for regenerating agents. Their healing activity was explained by a protective action on HBGF and an increase in HBGF bioavailability (10–12). In addition to their repair activity in craniotomy wounds, we observed a modification of the kinetics of inflammation (13). This was in keeping with in vitro observations that RGTA inhibited plasmin and neutrophil elastase activity (14, 15). As periodontitis is a disease in which comprehensive treatment should ideally combine control of inflammation and periodontal destruction with tissue repair promotion, we examined the effects of systemic administration of an RGTA (RGTA1507) in a highly reproducible hamster model of periodontitis.

[1] Correspondence: CNRS FRE 2412 Université Paris-12 Val de Marne, Av. du Général de Gaulle, 94000 Créteil, France. E-mail: saffar@odontologie.univ-paris5.fr

0892-6638/03/0017-0644 © FASEB

MATERIALS AND METHODS

RGTA synthesis

The RGTA used in this study was a carboxymethyl sulfate dextran prepared from a native T40 dextran (40 kDa; Pharmacia Fine Chemicals, Uppsala, Sweden) obtained as described previously (15). Sequential substitutions on any of the three hydroxylic groups (mainly in position 2) of the glucose residues of the dextran were carboxymethylations, followed by sulfation. The purified derivatized dextran was ultrafiltered and its chemical composition was determined by microanalysis, spectrophotometry, and proton nuclear magnetic resonance. With the RG1503 used in this study, the percentage of hydroxyl groups per glucose residue-bearing substitutions was 26% for methylcarboxylic acid and 74% for sulfate groups. This compound was selected because of its low anticomplement activity, its very low anticoagulant activity (4 IU/mg), and its ability to mimic in vitro interactions between heparin or heparan-sulfate proteoglycans and FGF-1 (11) or TGF-β (16).

Dose-effect study

Sixty male 6-wk-old golden hamsters (Centre d'élevage Dépré, St. Doulchard, France) were used in compliance with European Union recommendations on laboratory animal care. Food and water were given ad libitum. Ten animals randomly selected as controls at the start of the experiment received a standard rodent diet (U.A.R., Villemoisson, France) throughout the 12 wk experimental period. The other animals were given the high-carbohydrate Keyes 2000 diet (U.A.R., France) throughout the 12 wk to enhance bacterial plaque accumulation, thereby inducing periodontitis. Eight weeks later, the 50 hamsters with periodontitis were separated into five equal groups. One group received weekly intramuscular (i.m.) injections of saline for 4 wk (sham-treated group). The other groups were given one i.m. injection per week of RGTA in saline in a dose of 100 μg/kg (group D1), 400 μg/kg (group D2), 1.5 mg/kg (group D3), or 15 mg/kg (group D4). At the end of the 12 wk, five animals per group received an intraperitoneal (i.p.) injection of bromodeoxyuridine (BrdU) (60 mg/kg) (Sigma, St. Louis, MO, USA) and were killed 2 h later for assessment of cell proliferation. The animals were anesthetized with 8% chloral hydrate and exsanguinated by cardiac puncture through a thoracostomy.

Histological studies

The right mandibles of the killed animals were immediately removed, immersed for 24 h in cold (4°C) 40% ethanol, gradually dehydrated, embedded without prior demineralization in methyl methacrylate (Merck, Darmstadt, Germany), and polymerized at −20°C for 48 h. The blocks were coded to allow blind quantification and were processed for sectioning in a Polycut E microtome (Leica, Wetzlar, Germany). Serial 4 μ-thick sections were cut horizontally, i.e., perpendicularly to the molar root axis. The sections were sequentially stained with toluidine blue (pH 3.8) or processed for enzymohistochemistry (tartrate-resistant acid phosphatase [TRAP] and alkaline phosphatase, [ALP]) or immunohistochemistry (type III collagen and BrdU). TRAP, a marker of preosteoclasts and osteoclasts in the bone environment, was detected using hexazotised pararosanilin and naphthol ASTR phosphate. Nonosteoclastic acid phosphatase activity was inhibited by 50 mM L(+)-tartaric acid. Sections were lightly counterstained with toluidine blue (pH 3.8). ALP was detected by incubating the sections with naphthol ASTR phosphate and fast blue RR (pH 9). ALP was used to reveal osteogenic cells (preosteoblasts and osteoblasts). The fibrous component of the gingival connective tissue was stained by ALP. For type III collagen immunochemistry, the sections were decalcified (0.4 M EDTA) and treated with 0.05% pronase E (protease type XXV, Sigma). They were incubated first with a rabbit anti-rat polyclonal antibody (AB757, Chemicon International, Temecula, CA, USA) (dilution 1:50), with a secondary biotinylated antibody (goat anti-rabbit IgG) (Vector, Burlingame, CA, USA), and an avidin-biotin peroxidase complex (ABC Vectastain kit, Vector). Diaminobenzidine tetrahydrochloride (Sigma) was the chromogen. The sections were lightly counterstained with toluidine blue (pH 3.8). Negative controls were prepared using three methods: omission of the primary antibody, replacement of the primary antibody by rabbit nonimmune serum at the same dilution, and use of an irrelevant secondary antibody (horse antimouse IgG instead of goat anti-rabbit IgG). To reveal BrdU, the sections were treated first with 0.1% trypsin (Sigma), then with 2 M HCl to denature the DNA. After incubation with normal horse serum (Vector), the anti-BrdU antibody (Sigma) (1:1000) was applied, followed by the secondary antibody (horse antimouse IgG, Vector) (1:200). The subsequent steps and negative controls were as described above. A light toluidine blue counterstain was used.

Macroscopic bone measurements

52 6-wk-old hamsters were divided into three groups. Twelve animals were used as controls; the other 40 were given the Keyes 2000 diet throughout the 16 wk experimental period. After disease induction (8 wk), 20 animals were sham-treated and 20 received weekly RGTA injections (1.5 $mg \cdot kg^{-1} \cdot wk^{-1}$) for 8 wk. Two fluorescent dies were injected i.p.: *1)* calcein (30 mg/kg in saline containing 2% $NaHCO_3$, Sigma) 8 days before killing and *2)* demeclocyclin (30 mg/kg in saline, Sigma) 24 h before. The dies incorporated to calcifying bone matrix. When exposed to UV light, calcein was revealed in green and demeclocycline in yellow. The mandibles of these animals were processed as described previously.

After gingiva sampling, the maxilla were defleshed. The lingual aspect of the first molar was oriented under a Tessovar Photomacrographic Zoom System (Zeiss, Oberkochen, Germany) and photographed (magnification ×50). The cement-enamel junction and the alveolar bone crest were drawn on the photographs. These lines were joined at the distal and mesial aspects of the teeth, respectively. The area thus delimited, which gave an estimate of macroscopic bone loss, was measured.

Gelatinolytic activities

Immediately after the death of the animals, the gingiva surrounding the right and left maxillary molars was gently dissected out, transferred to Hank's balanced salt solution complemented with 1.5 mmol/L Ca^{2+} (Life Technologies, Stafford, TX, USA), and incubated at 37°C. The culture medium was sampled after 48 and 72 h and frozen (−20°C) until zymography. Gelatinases A (MMP-2) and B (MMP-9) were identified using 0.1% SDS polyacrylamide gels impregnated with 1 mg/mL type I gelatin. Protein standards were analyzed in parallel to determine the molecular weights of the lysis bands. To assign these bands to a proteinase class, the following reagents (all from Sigma) were added to the incubation buffer to inhibit protease migration: EDTA (15 mmol/L) or phenanthrolene (15 mmol/L) for metalloproteinases, phenylmethylsulfonyl fluoride (PMSF, 2 mmol/L) or 4-(2-aminoethyl)-benzene-sulfonyl fluoride, hydrochloride

(Pefablock, 2 mmol/L) for serine proteinases, and N-ethylmaleimide (2 mmol/L) for cysteine proteinases. The stained polyacrylamide gels were recorded with a video camera. The average area Ar (expressed in pixels) of lysis bands was measured semiautomatically by following its contour. The black and white images generated by the camera were converted to images in 256 shades of gray and analyzed using mathematical morphology software. Complete digestion of the substrate corresponded to gray level (gl) 255, and the absence of hydrolysis corresponded to gl 0. Enzyme activity was expressed in gelatinase activity units (GAU): GAU = Ar.gl.

Statistical analysis

Data were compared using nonparametric tests (Kruskal-Wallis test followed, if significant, by group comparisons with the Mann-Whitney U test). Differences were considered significant when P values were below 0.05. Data are given as means ± SE.

RESULTS

RGTA 1503 was well tolerated in all the doses and durations used in this study. Among the animals with periodontitis, the RGTA-treated animals did not differ from the sham-treated animals in physical health, behavior, or other studied parameters. No manifestations of periodontitis were seen in the healthy controls fed a normal diet.

RGTA induces dose-dependent gingival restoration (Table 1)

Pocket formation around the first molar was a consistent feature in the animals with periodontitis. Abundant bacterial plaque accumulated over the roots and filled the pockets, which were lined by pocket epithelium (PE) and populated by migrating polymorphonuclear leukocytes (PMN). Wide spaces separated the epithelial cells. Epithelial ridges extended deep within the underlying connective tissue, and connective projections were seen within the epithelium (**Fig. 1*a***). A zone of inflamed connective tissue (ICT) was visible immediately under the PE. This ICT was characterized by a paucity of fibers, an abundance of blood vessels, and PMN migration toward the pocket lumen (Fig. 1*a*). Periodontitis also affected alkaline phosphatase (ALP) content of the gingival connective tissue (Fig. 2*a*), which consistently expresses ALP (17).

RGTA-treated animals had milder manifestations despite persistent bacterial plaque. The PE was thicker and had narrower intercellular spaces than in the sham-treated animals. The ICT was less abundant, and the pocket tissues contained fewer PMNs (Fig. 1*b*). The epithelial ridges within the connective tissue were less numerous (Fig. 1*b*). The noninflamed connective tissue between the pocket and the alveolar bone was more fibrous. ALP expression in the gingival connective tissue was restored (**Fig. 2*b***). Although the total pocket surface area (PE + ICT) was similar in the two periodontitis groups (Table 1), the ratio of the two tissues was modified by RGTA treatment, with a significant increase of ~40% in groups D1, D2, and D3 compared with the sham-treated group. This increase was offset by a significant decrease in ICT in the RGTA-treated groups. The number of PMNs in the ICT was significantly reduced in group D1 only (−31%, $P<0.05$). The number of marginating PMNs was reduced in three treatment groups (−46% in D1 [$P<0.001$], −33% in D3 [$P<0.01$], and −25% in D4 [$P<0.01$]).

Type III collagen was strongly expressed in the gingival connective tissue from the healthy controls (Fig. 1*c*). In the sham-treated animals (Fig. 1*d*), weak and diffuse immunostaining in the gingival connective tissue contrasted with strong immunostaining in healthy areas of the mandible, indicating that weak gingival staining reflected paucity of collagen fibers. Some immunostaining was found along the PE basement membrane. In RGTA-treated animals (Fig. 1*e*), the staining was stronger along the basement membranes of the PE and vessels, as well as in the connective tissue. No immunostaining was seen in the osteoid tissue or osteoblasts. None of the procedures used

TABLE 1. *Changes in gingival inflammation markers*

	Pocket surface area (mm^2)[a]	Pocket epithelium (%)[b]	ICT (%)[b]	PMN in ICT (n/mm^2)	Marginating PMN (n/vessel)	$BrdU^+$ cells (N/mm^2)[c]
Healthy controls	—	—	—	—	—	—
Sham-treated animals with periodontitis	1.4 ± 0.2	33.4 ± 4.3	66.6 ± 4.3	4737 ± 602	5.5 ± 0.4	382 ± 39
100 μg/kg RGTA (D1)	1.6 ± 0.1	46.4 ± 2.9*	53.6 ± 2.9*	3229 ± 203	2.9 ± 0.2**	642 ± 57**
400 μg/kg RGTA (D2)	1.9 ± 0.2	46.9 ± 1.2**	53.1 ± 1.2**	4276 ± 232	4.4 ± 0.4	538 ± 51
1.5 mg/kg RGTA (D3)	1.4 ± 0.2	47.7 ± 3.4*	52.3 ± 3.4*	3906 ± 202*,+	3.7 ± 0.2**	1121 ± 84***
15 mg/kg RGTA (D4)	1.5 ± 0.1	40.7 ± 3.0	59.3 ± 3.0	3886 ± 365	4.1 ± 0.2*,++	636 ± 31**
Kruskal-Wallis test	H = 4.128 NS	H = 11.830 $P = 0.0187$	H = 11.830 $P = 0.0187$	H = 10.23 $P = 0.037$	H = 21.85 $P = 0.0002$	H = 30.04 $P < 0.0001$

[a] This parameter included pocket epithelium and inflamed connective tissue (ICT), around the first molar. [b] Expressed as the percentage of pocket tissues. [c] Count of BrdU-positive cells in the pocket epithelium (cells per mm^2 of pocket epithelium). ICT: inflamed connective tissue, PMN: polymorphonuclear leukocytes. * $P < 0.05$, ** $P < 0.01$, *** $P < 0.0005$ vs. the sham treated periodontitis group. + $P < 0.05$, ++ $P < 0.01$ vs. the D1 group.

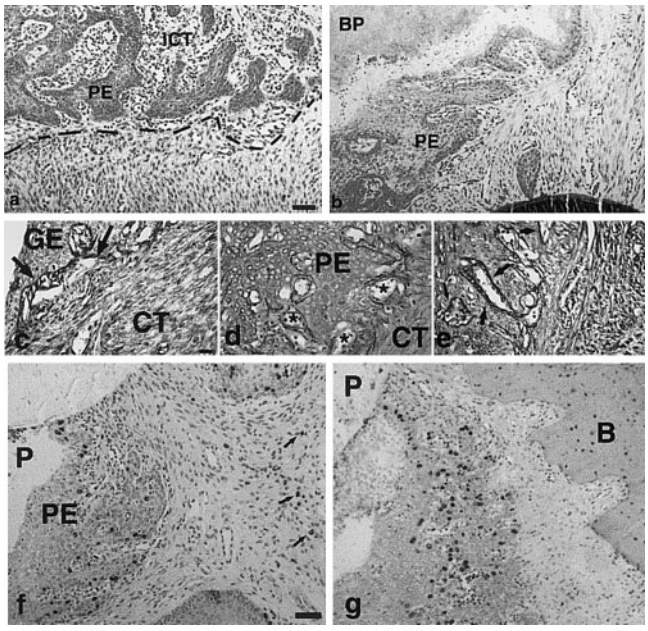

Figure 1. Effects of 6 wk RGTA treatment on gingival tissues. Manifestations of inflammation in sham-treated animal with periodontitis (*a*) and RGTA-treated (*b*). Toluidine blue staining. Bar = 50 μm. *a)* Numerous epithelial projections from the pocket epithelium (PE) are surrounded by disorganized connective tissue, which is highly vascularized and infiltrated by PMNs. The dotted line marks the boundary between the inflamed connective tissue (ICT) and healthy noninflamed connective tissue. *b)* The amount of ICT is small, as shown by the dotted line, despite the neighboring bacterial plaque (BP). The pocket epithelium is less convoluted. Type III collagen immunochemistry *c)* Control animal. *d)* Sham-treated animal with periodontitis *e)* RGTA-treated animal. Bar = 20 μm. *c)* Strong immunostaining at the interface between the gingival epithelium (GE) and the connective tissue (CT) (arrows). The staining is dense in the connective tissue, with positive fibers running parallel to the epithelium-connective tissue interface. *d)* The interface between pocket epithelium (PE) and connective tissue (*) is weakly stained, as is the connective tissue (CT). *e)* The basement membranes are strongly immunostained, as in the control sample (arrows). The marker is strongly expressed in the connective tissue, indicating restructuring of the gingiva. BrdU labeling: *f)* Sham-treated animal with periodontitis. *g)* RGTA-treated animal. Bar = 50 μm. Proliferating cells are located mostly in the pocket epithelium (PE) surrounding the roots. Few $BrdU^+$ cells (arrows) are seen in the gingival connective tissue. *g)* The number of proliferating cells in the PE is larger than in the sham-treated animal. The epithelium appears thicker. P: pocket lumen; B: bone.

showed staining in the negative control sections. In the sham-treated animals (Fig. 1*f*), there were few proliferating cells (most of which were in the PE), as shown by BrdU incorporation and immunostaining. No immunopositive cells were seen near the bone. In RGTA-treated animals (Fig. 1*g*), cell proliferation was increased in the PE, mainly along the basement membrane but also within the epithelium. Immunostained cells were seldom observed in the gingival tissue or along the alveolar bone. No immunostaining was seen in any of the negative control sections. $BrdU^+$ cell counts in the PE increased with all RGTA doses (Table 1). This increase was particularly marked in the D3 group, in which there were threefold as many BrdU-positive cells as in the sham-treated group ($P<0.0005$); the BrdU-positive cell count in the D3 group differed significantly ($P<0.001$) from those in the other three dose groups.

RG1503 induced dose-dependent protection of bone metabolism (Table 2)

In the healthy control animals, bone formation predominated in the reference bone segment (57% on average) and no resorption was found. In the sham-treated animals, a significant part of the reference bone segment showed resorption, whereas formation was seldom observed. RGTA had no effect on bone status in groups D1 and D2. In contrast, the two higher RGTA doses improved bone status, D3 (1.5 $mg \cdot kg^{-1} \cdot wk^{-1}$) more than D4. Compared with the sham-treated group, the resorption surface was reduced by 65% ($P<0.0005$) in group D3 and by 27% ($P<0.005$) in group D4; the two treatment groups differed significantly in this respect ($P<0.005$). The number of osteoclasts was reduced by 49% ($P<0.0005$) in group D3. The number of $TRAP^+$ preosteoclasts located near the bone surface was reduced markedly in group D3 (−61%, $P<0.0005$ vs. the sham-treated group) and more moderately in group D4 (−31%; $P<0.001$); the two groups differed significantly in this respect ($P<0.05$). In group D3, there was a 2.25-fold increase in the surface area of newly formed bone ($P<0.0005$ vs. the sham group), although this parameter remained lower than in the healthy control group ($P<0.005$). The D4 dose had no effect on this parameter, so that the D3 and D4 groups differed significantly ($P<0.05$). The disease did not modify the thickness of the layer of osteogenic ALP^+ cells covering the bone surface. RGTA treatment nearly doubled the thickness of this ALP^+ layer in group D3 ($P<0.0002$ compared with the sham-treated animals with periodontitis) and produced more modest thickening in group D4 (+41%, $P<0.01$ vs. the same group) (**Fig. 2**). We further assessed the effect of RGTA on bone formation by obtaining planimetry measurements of defleshed maxillae prepared after 8 wk of RGTA treatment with dose D3 (**Fig. 3**). Mean bone loss over the maxillary first molar was 0.96 ± 0.02 mm^2 in the controls and 1.34 ± 0.08 mm^2 in the sham-treated animals ($P<0.0001$). In the RGTA-treated animals, macroscopic bone loss was similar to that in the controls (1.02 ± 0.03 mm^2). The sham- and RGTA-treated groups differed significantly in this respect ($P<0.001$). Bone growth was intense in RGTA-treated animals (Fig. 3).

RGTA alters gingival gelatinase activities

The effects of RGTA on gingival gelatinase activities were evaluated by zymography of culture medium conditioned by gingival explants (Fig 4, top). After 48 h of culturing, control gingival explants generated gela-

TABLE 2. *Changes in resorption and formation parameters along the reference bone segment*[a]

	Resorption surface (%)	Osteoclasts (N/mm)	TRAP+ preosteoclasts (N/mm)	Formation surface (%)	ALP+ osteogenic layer (μm)
Healthy controls	0.5 ± 0.31	0.60 ± 0.04	10.71 ± 1.22	57.7 ± 2.9	33.2 ± 2.4
Sham-treated animals with periodontitis	41.26 ± 1.86	20.56 ± 0.99	32.22 ± 1.21	18.2 ± 1.1†	33.7 ± 1.7
100 μg/kg RGTA (D1)	37.64 ± 1.83	21.15 ± 1.26	29.33 ± 1.77	15.7 ± 1.6	33.8 ± 1.9
400 μg/kg RGTA (D2)	37.99 ± 4.44	20.88 ± 1.66	30.09 ± 1.82	20.1 ± 1.7	39.0 ± 1.5
1.5 mg/kg RGTA (D3)	14.41 ± 2.24***	10.56 ± 1.04***	12.61 ± 0.72***	41.1 ± 3.3****	61.3 ± 3.6****
15 mg/kg RGTA (D4)	29.94 ± 2.04^{++}	19.11 ± 0.99^{++}	22.06 ± 2.04$^{*,+}$	26.3 ± 3.1^{+++}	47.5 ± 2.1$^{**,+++}$
Kruskal-Wallis test	H = 46.08 $P < 0.0001$	H = 42.307 $P < 0.0001$	H = 44.637 $P < 0.0001$	H = 43.42 $P < 0.0001$	H = 33.0 $P < 0.0001$

[a] These parameters were measured on the periosteal aspect of the lingual cortex between the first and second molars, at constant magnification (×250). TRAP: tartrate-resistant acid phosphatase, ALP: alkaline phosphatase. † $P < 0.001$ vs. the control group. * $P < 0.005$, ** $P < 0.001$, *** $P < 0.0005$, **** $P < 0.0002$ vs. the sham-treated periodontitis group. $^{+}$ $P < 0.05$, $^{++}$ $P < 0.005$, $^{+++}$ $P < 0.001$ vs. the D3 group.

tinolytic activities seen as bands at 62 kDa (progelatinase A, proMMP-2), 58 kDa (gelatinase A, matrix metalloproteinase-2 [MMP-2], and 102 kDa (progelatinase B, proMMP-9). The intensities of these bands were increased considerably with conditioned media from sham-treated animals and, to a lesser extent, from RGTA-treated animals. All activities were suppressed by supplementing the incubation buffer with EDTA (15 mmol/L); none were affected by Pefablock (2 mmol/L) or N-ethylmaleimide (2 mmol/L). Gelatinolytic activities were normalized to tissue weight (**Fig. 4**, bottom). In 48 h cultures, gelatinolytic activity in the control group was 39×10^5 GAU of proMMP-2, 16×10^5 GAU of MMP-2, and 17×10^5 GAU of proMMP-9. MMP-9 activity was below the detection limit. In the sham-treated animals, all gelatinolytic activities were significantly higher than in the control group. The active form of MMP-9 remained undetectable in the sham group. RG1503 1.5 mg·kg^{-1}·wk^{-1} strongly reduced proMMP-2 (−46.5%, $P<0.001$) and proMMP-9 (−50%, $P<0.05$) activities. No change was found in the 58 kDa activated form of MMP-2. The same profile of gelatinase activities was obtained in 72 h cultures (not shown).

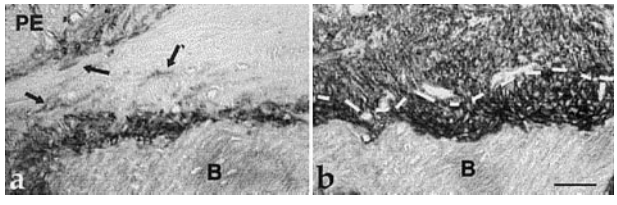

Figure 2. Effect of RGTA treatment on ALP^{+} activity in gingiva and bone. *a)* Sham-treated animal with periodontitis. *b)* RGTA-treated animal. Bar = 50 μm. *a)* In addition to the osteogenic layer, staining is seen in the gingival connective tissue (arrows). The layer of ALP-positive cells is thick and strongly stained. *b)* The gingival tissue is uniformly positive for ALP, but the staining is weaker. The dotted line indicates the boundaries between the osteogenic and gingival compartments. B: bone; PE: pocket epithelium.

DISCUSSION

The results presented above indicate that RG1503 had beneficial effects in the gingiva and bone in this model of periodontitis. Whereas periodontitis increases bone resorption and depresses bone formation (18), RG1503 had the opposite effects. The doses at which RG1503 was active varied across tissue compartments. RGTA improved gingival inflammation over a wide dose range, starting at the lowest dose used. In contrast, the greatest effect on bone was seen with the 1.5 mg·kg^{-1}·wk^{-1} dose (D3), so that the dose-effect curve had the same narrow bell shape found previously when RGTA was applied in microgram-amounts directly into skull defects (19). We showed that systemic administration of RGTA was as effective as local administration in enhancing regeneration of crushed muscle (20, 21). RGTA is analogous to heparan sulfates; intramuscular or intravenous injections of ^{3}H-labeled RGTA were followed by selective accumulation of radioactivity at injured sites (20), an effect reported with ^{3}H-heparin (22). Similar to heparan sulfates, RGTAs attach to the heparin binding sites of various ECM proteins exposed after heparan degradation by heparanase activated by tissue injury (23). However, RGTAs share with other dextran derivatives a lack of susceptibility to heparanase. When bound to ECM proteins, RGTAs probably protect these proteins against degradation and may neutralize molecules responsible for tissue destruction (14, 15). ECM-bound RGTA most likely binds to and protects HBGF. By a mechanism of simple competition, excess RGTA may remain unbound to the ECM and exit the tissue to the bloodstream, removing HBGF from its presumed natural storage sites and thereby delaying the healing process. This may explain the narrow bell shape of the dose-effect curve of RGTA. Increasing the duration of treatment (to 8 wk) with the most effective dose of RGTA returned the alveolar processes to a state very similar to that seen in the healthy controls, a remarkable finding given that the animals were fed the high-carbohydrate diet through-

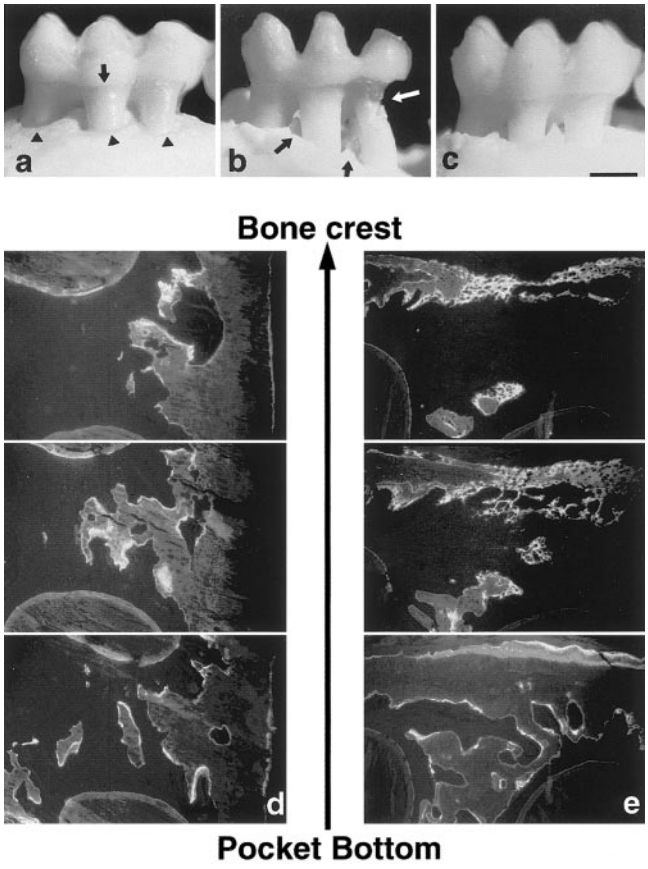

Figure 3. Effect of RGTA treatment on macroscopic bone loss and dynamics of repair. Bone loss on the palatal aspect of the first maxillary molar. *a)* Control animal. *b)* Sham-treated animal with periodontitis. *c)* RGTA-treated animal (after 8 wk, 1.5 $mg \cdot kg^{-1} \cdot wk^{-1}$). Bar = 1 mm. *a)* Root denudation is minimal. Alveolar bone crest contours (arrowheads) are smooth and regular. The arrows point to the cement-enamel junction. *b).* Bone loss is extensive, particularly at the distal root of the tooth (white arrow). The bone crest is irregular, and there are through and through (class III) furca lesions (black arrows), which indicate advanced disease. Note the carious lesion on the distal aspect of the tooth, a cofactor in bacteria accumulation. *c)* Bone loss is minimal, resembling that in controls, but the crest contour is somewhat irregular. Kinetics of new bone deposition (assessed by fluorescent labelings). It was spatially appreciated by viewing 3 sections, 40 μm apart, from pocket bottom to bone crest. *d)* Sham-treated periodontitis hamster. At each level some bone formation occurred. However it was sparse and of low extent (the labels were localized) and of short duration (absence of double labeling). *e)* RGTA-treated animal. Bone formation was extensive. Bottom: reparative bone formation was located on periosteal aspect of the cortex. The first label (green) was large, sign of a strong reaction, in contrast the second label (yellow) was thin, indicating a comparatively weak formative reaction at the time of injection. Center: the two labels were wide showing a strong reaction lasting during the interval between the dye injections (7 days). The amount of bone matrix mineralizing at each time point was great. Top: the amount of mineralizing matrix was low 8 days before death. In contrast, the day before death, it was considerable. These data demonstrate that the alveolar bone destroyed at a former time is progressively restored from the base of the pocket. Its growth is rapid (width of the labels) and continuous, suggesting a long-lasting effect of the treatment. The abundance of bone formed is congruent with alveolar bone macroscopic aspect.

out the 16 wk experimental period. These results are another illustration of the potent effects of RGTA, already reported in various models of tissue damage (19, 21, 24).

RGTA affected gingival inflammation. Although the surface area of pocket tissues was not modified by RGTA, the ratio between these tissues was changed. Thickening of the PE, which reflects epithelial cell proliferation, and narrowing of intercellular spaces indicate strengthening of the epithelial barrier. Given that epithelial cells are the first barrier against pocket bacteria and their products (25), it is reasonable to assume that this effect protects the underlying tissues. The epithelial proliferative response noted in our study is in line with previous reports that RGTA enhanced epithelial cell proliferation and migration and accelerated wound closure in models of cutaneous and corneal ulcer repair (26, 27). The concomitant reduction in ICT in our study was another indicator of gingival repair. The deposition of a thick layer of type III collagen under the PE basement membrane probably helped to stabilize the epithelial junction by anchoring the basal cells more firmly to their basement membrane. Members of the RGTA family have been shown to modulate collagen synthesis in vitro. Collagen production impaired by culturing or irradiation was completely corrected by RG1503, via an effect related to TGFβ1 distribution (16, 28, 29). In vivo, RGTA enhanced deposition of types I and III collagen within the provisional matrix that filled craniotomy defects before the onset of bone formation (30). The increased production of type III collagen in noninflamed connective tissue and the expression of ALP in gingival connective tissue were further evidence of gingival restructuring. The reduction in PMN recruitment may indicate that RGTA influenced the chemotactic gradient governing PMN migration toward plaque bacteria. We previously

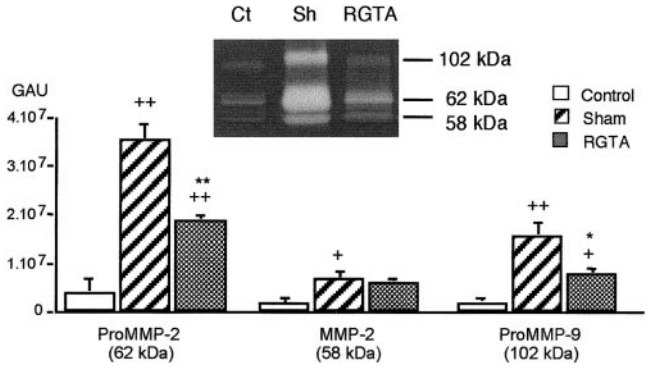

Figure 4. Effect of RGTA administration on gelatinolytic activities. Top: Gelatin zymograms of gingival explant media after 48 h of incubation. Ct: incubation medium from a control animal. Sh: sham-treated animal. RGTA: RGTA-treated animal (1.5 ·kg/wk for 8 wk). Note the particularly strong staining for proMMP-2 (62 kDa) and proMMP-9 (102 kDa) in the sham-treated animals. RGTA treatment reduced the intensity of the staining. Bottom: Densitometric analysis of gelatinolytic activities. GAU: gelatinolytic activity units. $+P < 0.01$, $++P < 0.001$ vs. controls; $*P < 0.05$, $**P < 0.001$ vs. sham.

found that RGTA treatment reduced PMN recruitment to craniotomy defects and shortened the acute phase of inflammation (J. L. Saffar, unpublished results). The reduced PMN migration may have contributed to gingival restructuring, given that PMNs cause damage to periodontal tissues as they migrate toward the pocket. RGTA has anti-inflammatory properties, exerted through inhibition of plasmin and neutrophil elastase activity (14, 15). Our study extends the anti-inflammatory repertoire of RGTA to MMP activity: we found that RGTA had a strong effect on gelatinase activities in inflamed gingival tissue. MMP-2, known to contribute to periodontal tissue destruction (31), was found in both its inactivated and active forms, whereas MMP-9 was detected with our assay only in its inactive form (proMMP-9), regardless of gingival status. RGTA treatment reduced the amount of proMMP-2 but did not influence the amount of its active form. RGTA may influence the expression and/or secretion of MMP-2, which is secreted as a proenzyme (32). The concomitant decrease in proMMP-9 in the treated animals suggests that RGTA may similarly target the expression and/or secretion of this proenzyme. RGTA may enhance the release of TIMP, inactivating gelatinase A and B pro-forms. Periodontitis is characterized by a 60–70% decrease in gingival collagen (33). Fibrillar collagens are mainly degraded by collagenases belonging to the MMP family (34), particularly collagenase 1 (MMP-1) and PMN-type collagenase (MMP-8). MMP-2 has strong collagenolytic effects: in vivo, overexpression and activation of MMP-2 result in marked degradation of skin fibrillar collagen, particularly type III collagen (35). In this study, the decrease in MMP-2 after RGTA treatment fits in well with the increased type III collagen content and with the morphological fibrillar restructuring of gingival connective tissue. MMP-2 has been shown to influence epithelial cell migration (36), playing a pivotal role in PE proliferation and migration along dental roots. In keeping with these properties, strong MMP-2 expression has been found in areas of inflamed PE with local invasion of underlying connective tissue (37). The reduced MMP-2 expression after RGTA treatment in our study is congruent with the decrease in PE ridges.

The gingival improvement was associated with a reduction in alveolar bone resorption. After 1 month of RGTA treatment, the number of osteoclasts destroying alveolar bone was cut by half, indicating a potent effect on osteoclast differentiation. This was related to a reduction in TRAP+ preosteoclasts, indicating an impairment of either recruitment from the circulation or differentiation of these cells. This is in keeping with our previous finding of modified osteoclast resorption at the edges of craniotomy defects (13). Also relevant is that MMP-2 and MMP-9 are involved in bone resorption and that MMP inhibitors reduce bone resorption (37).

Restoring the coupling between bone formation and bone resorption is essential to improve the bone lesions associated with periodontitis. In our study, the same doses of RGTA enhanced bone formation and inhibited bone resorption. RGTA increased the extent of bone formation and thickened the osteogenic layer, reflecting a potent action on osteogenic cells. In models of bone healing, RGTA strongly enhanced osteoblast proliferation and phenotype expression (19, 30, 38). The absence of $BrdU^+$ cells along the bone surface suggests that osteogenic cell proliferation was an early effect of RGTA treatment. In the craniotomy model, the formation of a dense network of type III collagen is concomitant of osteogenic cell differentiation (30). The increase in type III collagen content of adjacent gingival tissue in our study is noteworthy in this respect. The marked recruitment of osteoprogenitor cells explained the dramatic gain in maxillary alveolar bone in the animals treated for 2 months. These data strongly suggest that RGTA treatment induced a two-phase reaction. The first phase was suppression of gingival inflammation and induction of tissue restructuring and of osteoprogenitor cell recruitment and proliferation over the formerly destroyed bone. In the second phase, RGTA enhanced restoration of destroyed bone via expression of the phenotype of recruited osteoprogenitor cells. As analogs of heparan sulfate proteoglycans, RGTA may interact with a variety of heparin binding molecules of the ECM or released in the tissues. These interactions may neutralize molecules responsible for tissue destruction, and/or enhance the expression of healing promoters. The exact mechanisms of action as well as the structure–activity relationships of RGTA would need to be more explicated, but this in vivo model is too tedious to screen the most efficient structures. In a previous study we had already shown that both sulfate and carboxymethyl groups were required for biological activities. Indeed, in craniotomy defects in which RGTA strongly enhanced bone formation, bone healing did not occur when nonsulfated carboxymethyl dextran or dextran sulfate were used (39). Another limiting factor was the size of the polymer, since a 10 kDa dextran adequately substituted was ineffective in inducing bone formation. In conclusion, the effects of RGTA in this hamster model of periodontitis hold promise for the development of therapeutic agents capable of enhancing protection and repair of periodontal tissues damaged by periodontal pathogens. FJ

This study was supported by University Paris-5 (Axe d'excellence), by University Paris 12, the CNRS, and Naturalia et Biologia.

REFERENCES

1. Albandar, J. M., and Rams, T. E. (2002) Global epidemiology of periodontal diseases: an overview. *Periodontol. 2000* **29**, 7-10
2. Scannapieco, F. A., and Genco, R. J. (1999) Association of periodontal infections with atherosclerotic and pulmonary diseases. *J. Period. Res.* **34,** 340–345
3. Matsuki, Y., Yamamoto, T., and Hara, K. (1992) Detection of inflammatory cytokine messenger RNA (mRNA)-expressing

cells in human inflamed gingiva by combined in situ hybridization and immunohistochemistry. *Immunology* **76,** 42–47
4. Kornman, K. S., Crane, A., Wang, H. Y., di Giovine, F. S., Newman, M. G., Pirk, F. W., Wilson, T. G., Higginbottom, F. L., and Duff, G. W. (1997) The interleukin-1 genotype as a severity factor in adult periodontal disease. *J. Clin. Periodontol.* **24,** 72–77
5. Lasfargues, J. J., and Saffar, J. L. (1983) Effect of indomethacin on bone destruction during experimental periodontal disease in the hamster. *J. Period. Res.* **18,** 110–117
6. Reddy, M. S., Palcanis, K. G., Barnett, M. L., Haigh, S., Charles, C. H., and Jeffcoat, M. K. (1993) Efficacy of meclofenamate sodium (Meclomen®) in the treatment of rapidly progressive periodontitis. *J. Clin. Periodontol.* **20,** 635–640
7. Paquette, D. W., Fiorellini, J. P., Martuscelli, G., Oringer, R. J., Howell, T. H., McCullough, J. R., Reasner, D. S., and Williams, R. C. (1997) Enantiospecific inhibition of ligature-induced periodontitis in beagles with topical (S)-ketoprofen. *J. Clin. Periodontol.* **24,** 521–528
8. Chang, K. M., Ramamurthy, N. S., McNamara, T. F., Evans, R. T., Klausen, B., Murray, P. A., and Golub, L. M. (1994) Tetracyclines inhibit porphyromonas gingivalis-induced alveolar bone loss in rats by a non-antimicrobial mechanism. *J. Period. Res.* **29,** 242–249
9. Golub, L. M., Lee, H. M., Greenwald, R. A., Ryan, M. E., Sorsa, T., Salo, T., and Giannobile, W. V. (1997) A matrix metalloproteinase inhibitor reduces bone-type collagen degradation fragments and specific collagenases in gingival crevicular fluid during adult periodontitis. *Inflamm. Res.* **46,** 310–319
10. Tardieu, M., Gamby, C., Avramoglou, T., Jozefonvicz, J., and Barritault, D. (1989) Biological and binding studies of acidic fibroblast growth factor in the presence of substituted dextran. *J. Biomater. Sci. Polymer Ed.* **1,** 63–70
11. Tardieu, M., Slaoui, F., Josefonvicz, J., Courty, J., Gamby, C., and Barritault, D. (1992) Derivatized dextrans mimic heparin as stabilizers, potentiators, and protectors of acidic or basic FGF. *J. Cell. Physiol.* **150,** 194–203
12. Meddahi, A., Benoit, J., Ayoub, N., Sézeur, A., and Barritault, D. (1996) Heparin-like polymers derived from dextran enhance colonic anastomosis resistance to leakage. *J. Biomed. Mater. Res.* **31,** 293–297
13. Colombier, M. L., Lafont, J., Blanquaert, F., Carruelle, J. P., Barritault, D., and Saffar, J. L. (1999) A single low dose of RGTA, a new healing agent, hastens wound maturation and enhances bone deposition in rat craniotomy defects. *Cells, Tissues. Organs* **164,** 131–140
14. Meddahi, A., Lemdjabar, H., Caruelle, J. P., Barritault, D., and Hornebeck, W. (1996) FGF protection and inhibition of human neutrophil elastase by carboxymethyl benzylamide sulfonate dextran derivatives. *Int. J. Biol. Macromol.* **18,** 141–145
15. Ledoux D., Papy-Garcia, D., Escartin, Q., Sagot, M. A., Cao, Y., Barritault, D., Courtois, J., Hornebeck, W., and Caruelle, J. P. (2000) Human plasmin enzymatic activity is inhibited by chemically modified dextrans. *J. Biol. Chem.* **275**, 29383-29390
16. Alexakis, C., Guettoufi, A., Mestries, P., Strup, C., Mathe, D., Barbaud, C., Barritault, D., Caruelle, J. P., and Kern, P. (2001) Heparan mimetic regulates collagen expression and TGF-beta1 distribution in gamma-irradiated human intestinal smooth muscle cells. *FASEB J.* **15,** 1546–1554
17. Ivanovski, S., Li, H., Hasse, H. R., and Barthold, P. M. (2001) Expression of bone associated macromolecules by gingival and periodontal ligament fibroblasts. *J. Periodont. Res.* **36,** 131–141
18. Baron, R., and Saffar, J. L. (1978) A quantitative study of bone remodeling during experimental disease in the golden hamster. *J. Period. Res.* **13,** 309–315
19. Blanquaert, F., Saffar, J. L., Colombier, M. L., Carpentier, G., Barritault, D., and Caruelle, J. P. (1995) Heparan-like molecules induce the repair of skull defects. *Bone* **17,** 499–506
20. Meddahi, A., Brée, F., Papy-Garcia, D., Gautron, J., Rosso, Y., Barritault, D., and Caruelle, J. P. (2002) Pharmacological studies of RGTA11, a heparan sulfate mimetic polymer, efficient on muscle regeneration. *J. Biomed. Mater. Res.* **62,**525-531
21. Desgranges, P., Barbaud, C., Caruelle, J. P., Barritault, D., and Gautron, J. (1999) A substituted dextran enhances muscle fiber survival and regeneration in ischemic and denervated rat EDL muscle. *FASEB J.* **13,** 761–766
22. Medalion, B., Merin, G., Aingorn, H., Miao, H. Q., Nagler, A., Elami, A., Ishai-Michaeli, R., and Vlodavsky, I. (1997) Endogenous basic fibroblast growth factor displaced by heparin from the lumenal surface of human blood vessels is preferentially sequestered by injured regions of the vessel wall. *Circulation* **95,** 1853–1862
23. Vlodavsky, I., Friedmann, Y., Elkin, M., Aingorn, H., Atzmon, R., Ishai-Michaeli, R., Bitan, M., Pappo, O., Peretz, T., Michal, I., et al. (1999) Mammalian heparanase: gene cloning, expression and function in tumor progression and metastasis. *Nat. Med.* **5,** 793–802
24. Yamauchi, H., Desgranges, P., Lecerf, L., Papy-Garcia, D., Tournaire, M. C., Moczar, M., Loisance, D., and Barritault, D. (2000) New agents for the treatment of infarcted myocardium. *FASEB J.* **14,** 2133–2134
25. Okada, H., and Murakami, S. (1998) Cytokine expression in periodontal health and disease. *Crit. Rev. Oral Biol. Med.* **9,** 248–266
26. Meddahi, A., Blanquaert, F., Saffar, J. L., Colombier, M. L., Caruelle, J. P., Josefonvicz, J., and Barritault, D. (1994) New approaches to tissue regeneration and repair. *Pathol. Res. Pract.* **190,** 923–928
27. Fredj-Reygrobellet, D., Hristova, D. L., Ettaiche, M., Meddahi, A., Jozefonwicz, J., and Barritault, D. (1994) CMDBS, functional analogue of heparin sulfate as a new class of corneal ulcer healing agents. *Ophthalmic Res.* **26,** 325–331
28. Mestries, P., Borchiellini, C., Barbaud, C., Duchesnay, A., Escartin, Q., Barritault, D., Caruelle, J. P., and Kern, P. (1998) Chemically modified dextrans modulate expression of collagen phenotype by cultured smooth muscle cells in relation to the degree of carboxymethyl, benzylamide, and sulfation substitutions. *J. Biomed. Mater. Res.* **42,** 286–294
29. Mestries, P., Alexakis, C., Papy-Garcia, D., Duchesnay, A., Barritault, D., Caruelle, J. P., and Kern, P. (2001) Specific RGTA increases collagen V expression by cultured aortic smooth muscle cells via activation and protection of transforming growth factor-beta1. *Matrix Biol.* **20,** 171–181
30. Lafont, J., Baroukh, B., Berdal, A., Colombier, M. L., Barritault, D., Caruelle, J. P., and Saffar, J. L. (1998) RGTA11, a new heating agent, triggers developmental events during healing of craniotomy defects in adult rats. *Growth Factors* **16,** 23–38
31. Dahan, M., Nawrocki, B., Elkaim, R., Soell, M., Bolcato-Bellemin, A. L., Birembaut, P., and Tenenbaum, H. (2001) Expression of matrix metalloproteinases in healthy and diseased human gingiva. *J. Clin. Periodontol.* **28,** 128–136
32. Beranger, J. Y., Godeau, G., Frances, C., Robert, L., and Hornebeck, W. (1994) Presence of gelatinase A at the plasma membrane of human skin fibroblasts. Influence of cytokines and growth factors on cell-associated metalloendopeptidase levels. *Cell Biol. Int.* **18,** 715–722
33. Seguier, S., Godeau, G., and Brousse, N. (2000) Collagen fibers and inflammatory cells in healthy and diseased human gingival tissues. a comparative and quantitative study by immunohistochemistry and automated image analysis. *J. Periodontol.* **71,** 1079–1085
34. Birkedal-Hansen, H. (1995) Proteolytic remodeling of extracellular matrix. *Curr. Opin. Cell Biol.* **7,** 728–735
35. Berton, A., Godeau, G., Emonard, H., Baba, K., Bellon, P., Hornebeck, W., and Bellon, G. (2000) *Matrix Biol.* **19,** 139–148
36. Mäkelä, M., Larjava, H., Pirila, E., Maisi, P., Salo, T., Sorsa, T., and Uitto, V. J. (1999) Matrix metalloproteinase 2 (gelatinase A) is related to migration of keratinocytes. *Exp. Cell Res.* **251,** 67–78
37. Kusano, K., Miyaura, C., Inada, M., Tamura, T., Ito, A., Nagase, H., Kamoi, K., and Suda, T. (1998) Regulation of matrix metalloproteinases (MMP-2, -3, -9, and -13) by interleukin-1 and interleukin-6 in mouse calvaria: Association of MMP induction with bone resorption. *Endocrinology* **139,** 1338–1345
38. Albo, D., Long, C., Jhala, N., Atkinson, B., Granik, M. S., Wang, T., Meddahi, A., Barritault, D., and Solomon, M. P. (1996) Modulation of cranial bone healing with a heparin-like dextran derivative. *J. Craniofac. Surg.* **7,** 19–22
39. Lafont, J., Baroukh, B., Meddahi, A., Caruelle, J. P., Barritault, D., and Saffar, J. L. (1994) Derivatized dextrans (CMDBS) as promoters of bone healing. Factors influencing their effectiveness. *Cells Mater* **4,** 219–230

Received for publication July 24, 2002.
Accepted for publication December 17, 2002.